ISSN 0016-7932, Geomagnetism and Aeronomy, 2023, Vol. 63, No. 6, pp. 757–769. © Pleiades Publishing, Ltd., 2023.
Russian Text © The Author(s), 2023, published in Geomagnetizm i Aeronomiya, 2023, Vol. 63, No. 6, pp. 775–787.

Phenomena in the High-Latitude *F* Region of the Ionosphere under the Effect of Powerful HF Radio Waves at Frequencies above the Critical One of the *F*2 Layer

N. F. Blagoveshchenskaya[a], *, A. S. Kalishin[a], T. D. Borisova[a], I. M. Egorov[a], and G. A. Zagorskiy[a]

[a] *Arctic and Antarctic Research Institute of Roshydromet, St. Petersburg, 199397 Russia*

**e-mail: nataly@aari.nw.ru*

Received March 2, 2023; revised April 2, 2023; accepted May 25, 2023

Abstract—In this paper, we present the results of experimental studies of phenomena in the high-latitude upper (*F*-region) ionosphere caused by the impact of high-power HF radio waves of ordinary (O-mode) polarization at heating frequencies f_H that significantly exceed the critical frequency of the *F*2 layer ($f_H - foF2 = 0.9–1.1$ MHz). The results are based on experimental data obtained at the EISCAT/Heating HF heating facility in Tromsø, northern Norway (69.6° N, 19.2° E). In the experiments, a high-power HF radio wave of the O-polarization range was emitted in the direction of the magnetic zenith with a maximum effective radiation power of 350–550 MW. It was found for the first time that under conditions when a powerful HF radio wave of the O-polarization was not reflected from the ionosphere, ducts of increased electron density *Ne* are formed, and small-scale artificial ionospheric inhomogeneities and narrow-band (within a ±1-kHz band relative to the heating frequency) artificial radio emission of the ionosphere that are recorded at a distance of ~1200 km from the heating facility are generated. The characteristics of small-scale artificial ionospheric irregularities and the spectral structure of artificial radio emission of the ionosphere with alternative O/X heating to the magnetic zenith at frequencies significantly exceeding the critical frequency of the *F*2 layer are compared. It was established that, in general, their behavior has the same character, but the evolution of the development of the considered phenomena during O and X heating is different.

DOI: 10.1134/S0016793223600467

1. INTRODUCTION

The study of artificial ionospheric turbulence and plasma waves under the effect of high-power HF radio waves on the ionosphere is one of the actively developed areas of research in the physics of the ionosphere. In experimental studies to modify the upper (*F*-region) ionosphere, high-power HF radio waves (pump waves) of ordinary (O-mode) polarization are usually used on all HF heating facilities over the world. The pump wave of O-polarization at a radiation frequency below the critical frequency of the *F*2 layer ($f_H \le foF2$) effectively interacts with the ionospheric plasma at the altitudes of the upper hybrid resonance ($f_{UH}^2 = f_H^2 - fce^2$, where f_H and fce are the heating frequency and the electron gyrofrequency, respectively) and at the reflection altitude of a high-power HF radio wave ($f_O^2 = f_H^2$, where f_O is the local plasma frequency). This interaction leads to the excitation of thermal parametric (resonant) instability (Vaskov and Gurevich, 1975; Grach and Trakhtengerts, 1975) and parametric decay (striction) instability (Perkins et al., 1974; Hagfors et al., 1983; Stubbe et al., 1992, 1996; Kuo, 2014), which cause the generation of various phenomena in the upper ionosphere. The most important of them include an increase in the temperature of electrons, the generation of artificial ionospheric irregularities and artificial radio emission of the ionosphere (within a band of ±100 kHz relative to the frequency of the heating signal), artificial optical radiation, and excitation of plasma waves. Experimental studies of the characteristics, behavior, and features of the generation of these phenomena were intensively carried out and are being carried out on all HF heating facilities located at middle and high latitudes, including Sura, Arecibo, EISCAT/Heating, SPEAR, and HAARP (see, for example, (Robinson, 1989; Gurevich, 2007; Yeoman et al., 2007; Stubbe et al., 1996; Frolov, 2017; Blagoveshchenskaya, 2020).

The results of experiments carried out in recent years on the HAARP and EISCAT/Heating high-latitude HF heating facilities showed that at high effective radiation powers ($P_{eff} > 200$ MW), the generation of phenomena that are impossible at $P_{eff} \le 150–200$ MW is observed. These include the generation of additional layers in the ionosphere (Pedersen et al., 2010, 2011; Mishin et al., 2016) and the resumption of excitation of Langmuir and ion-acoustic plasma waves coexist-

ing with the generation of small-scale artificial ionospheric irregularities (SAIIs) (Ashrafi et al., 2007; Dhillon and Robinson, 2005; Blagoveshchenskaya et al., 2020).

In recent years, according to the results of numerous experiments performed by AARI specialists on the EISCAT/Heating HF heating facility, it was found that the impact on the high-latitude *F*-region of the ionosphere by powerful HF radio waves of extraordinary (X-mode) polarization in the direction of the magnetic zenith causes the generation of various phenomena, such as SAII, optical radiation in the red and green lines of atomic oxygen, narrow-band (within a band of ±1 kHz relative to the frequency f_H) artificial radio emission of the ionosphere, and excitation of Langmuir and ion-acoustic plasma waves (Blagoveshchenskaya et al., 2011, 2014, 2015, 2020, 2022; Kalishin et al., 2021; Kalishin et al., 2021, 2022; Blagoveshchenskaya, 2020). The excitation of various intense phenomena during X-heating was unexpected and was considered fundamentally impossible since the X-wave does not reach resonant altitudes in the ionosphere. This is due to its reflection at a altitude with a local plasma frequency $f_p^2 = f_H (f_H - fce)$, which is lower than both the O-wave reflection altitude and the altitude of the upper hybrid resonance. Furthermore, it should be emphasized that during X-heating, various phenomena in the *F*2-layer of the ionosphere are excited both at frequencies below the critical frequency of the *F*2 layer ($f_H \le foF2$), as is observed during O-heating, and at heating frequencies above the critical frequency ($f_H > foF2$) (Blagoveshchenskaya et al., 2022, 2018; Blagoveshchenskaya et al., 2011, 2015; Kalishin et al., 2022).

This research is aimed at studying the phenomena in the high-latitude upper (*F*-region) ionosphere at high effective radiation powers ($P_{eff} \sim 350$–550 MW) that are caused by the impact of high-power HF radio waves of O-polarization at frequencies significantly exceeding the critical frequency of the *F*2 layer ($f_H - foF2 = 0.9$–1.1 MHz), i.e., under heating conditions when the O-wave was not reflected from the ionosphere. The characteristics and time evolution of large-scale formations oriented along the magnetic field with an increased electron density (*Ne* ducts), small-scale artificial ionospheric inhomogeneities (SAIIs), and the spectral structure of narrow-band artificial ionospheric radio emission (NAIRE) are considered in detail for these conditions. The characteristics of the *Ne* ducts, SAII, and the spectral structure of the NAIRE are compared for alternative O-/X-heating to the magnetic zenith at frequencies significantly exceeding the critical frequency of the *F*2 layer.

2. EXPERIMENTAL

Experiments on the impact of high-power HF radio waves were carried out on the HF-heating EISCAT/Heating facility located near Tromsø, northern Norway (69.6° N, 19.2° E; $I = 78°$), which has no analogues in Russia both in terms of its technical characteristics and geographic location. The description and technical characteristics of the facility are given in (Rietveld et al., 2016). Here, we consider the results of an experiment on October 28, 2015 when a powerful HF radio wave was emitted into the magnetic zenith (12° south of the vertical) onto a phased antenna array 1 (PAR 1) with a beam width of 5°–6° (at the level of 3 dB). Alternative O/C heating from 1330 to 1400 UT was carried out at a frequency of $f_H = 7.953$ MHz in cycles of 10-min heating and 5-min pause at an effective radiation power of $P_{eff} = 550$ MW. From 1500 to 1530 UT, O/X heating was carried out at a frequency of $f_H = 6.77$ MHz at $P_{eff} = 350$ MW.

The EISCAT/Heating facility is spatially aligned with the EISCAT 930-MHz incoherent scatter (IS) radar (EISCAT UHF radar) (Rishbeth and van Eyken, 1993). During the experiment, the IS radar carried out measurements in the direction of the magnetic field in Tromsø, i.e., in the direction of the emission of a powerful HF radio wave. To analyze and interpret the results of the experiment, we used data on the altitude-time distribution of ionospheric plasma parameters (electron density *Ne* and temperature *Te*), as well as the power of heat-enhanced plasma and ion lines (HF-enhanced plasma and ion lines or HFPL and HFIL, respectively) in the IS radar spectra, the appearance of which is a direct indication of the excitation of longitudinal plasma waves (Langmuir and ion-acoustic). IS radar data were processed using the GUISDAP package, version 8.7 (Grand Unified Incoherent Scatter Design and Analysis Package) (Lehtinen and Huuskonen, 1996).

The characteristics of SAIIs excited by a powerful HF radio wave of O- or X-polarization were determined from measurements of the CUTLASS (SuperDARN) coherent HF radar in Hankasalmi, Finland (62.3° N, 26.6° E) that is located south of the heating facility (Lester et al., 2004). The measurements were carried out almost simultaneously at five frequencies of $f \sim 11.5$, 13.2, 16.2, 18, and 20 MHz, which provided the diagnostics of SAIIs with dimensions across the magnetic field of $l_\perp = 7.5$–13 m ($l_\perp = c/2f$, where f is the radar frequency). Radiation was carried out in the direction of an artificially disturbed region of the ionosphere above Tromsø, corresponding to beam 5. The time resolution was 3 s. The range gate was 15 km while the "first gate" started from a range of 480 km. Consequently, the "gate" numbers of from 20 to 50 correspond to the range from 780 to 1230 km, in which the signals scattered by SAIIs were registered.

NAIRE was registered at the AARI Gorkovskaya research station (60.27° N, 29.38° E) remote at a distance of ~1200 km from the heating facility. The heating signal was recorded using a decameter-range spectrum analyzer developed based on an IC-R75 radio

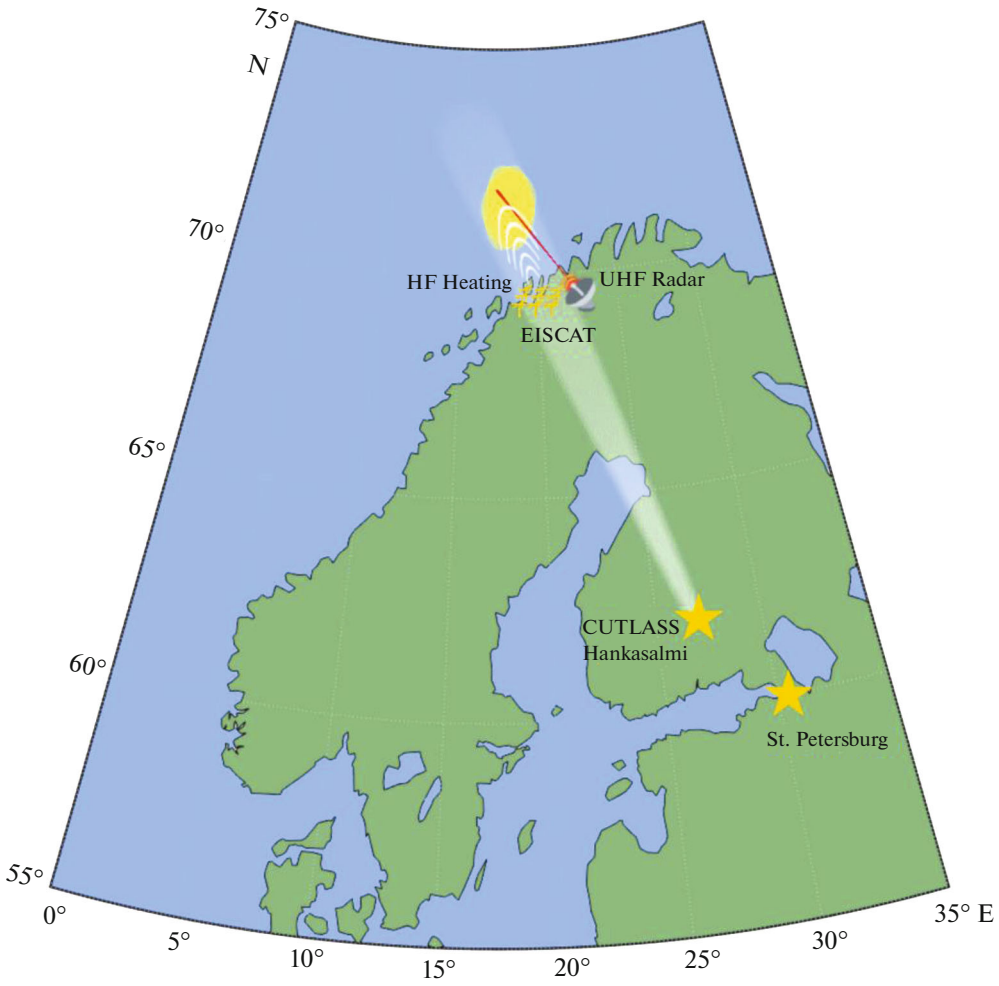

Fig. 1. A schematic map of the geometry of the experiment that shows the location of the HF-heating EISCAT/Heating facility and the incoherent scattering radar (EISCAT UHF radar), the CUTLASS radar in Hankasalmi, and the equipment for registering NAIRE near St. Petersburg.

receiver. A brief description of the receiving complex for registering NAIRE is given in (Kalishin et al., 2021). Radio signals were received using an antenna of the double horizontal rhombus type that was EISCAT/Heating oriented.

The state of the ionosphere was controlled by an ionosonde in Tromsø, which ensured the receipt of ionograms of vertical sounding of the ionosphere every 2 min. The map-scheme of the geometry of the experiment is shown in Fig. 1.

3. RESULTS

3.1. Experiment at a Heating Frequency of $f_H = 6.77$ MHz

Figure 2 shows the altitude–time distribution of electron density *Ne* and electron temperature *Te*, the behavior of *Ne* and *Te* at fixed altitudes according to measurements of the incoherent scattering radar, the NAIRE spectrogram, and variations of the critical frequencies of the *F*2 layer on October 28, 2015 from 1500 to 1530 UT with alternative O/X heating at f_H = 6.77 MHz. Figure 3 shows the powers of the signals scattered by SAIIs in dB (power, dB) at frequencies of $f \sim$ 11.5, 13.2, 16.2, and 18 MHz from CUTLASS observations for the same time interval. The data are given in the range (Range gate)-world time, UT coordinates.

The emission of a high-power O-polarized HF radio wave began at 1501 UT when the critical frequency of the *F*2 layer was *foF*2 = 5.9 MHz, which gradually decreased to *foF*2 = 5.6 MHz by the end of the X-heating cycle at 1526 UT. Thus, during the experiment, a heating frequency of f_H = 6.77 MHz exceeded *foF*2 by ~0.9–1.2 MHz, which indicates that both the powerful O-polarization wave in the 1501–1511 UT cycle and the X-wave in the 1516–1526 UT cycle did not reflect from the ionosphere. As follows from Fig. 2, in the O-heating cycle after turning on the heating stand, an increase in *Te* from 1500 K to 2000 K

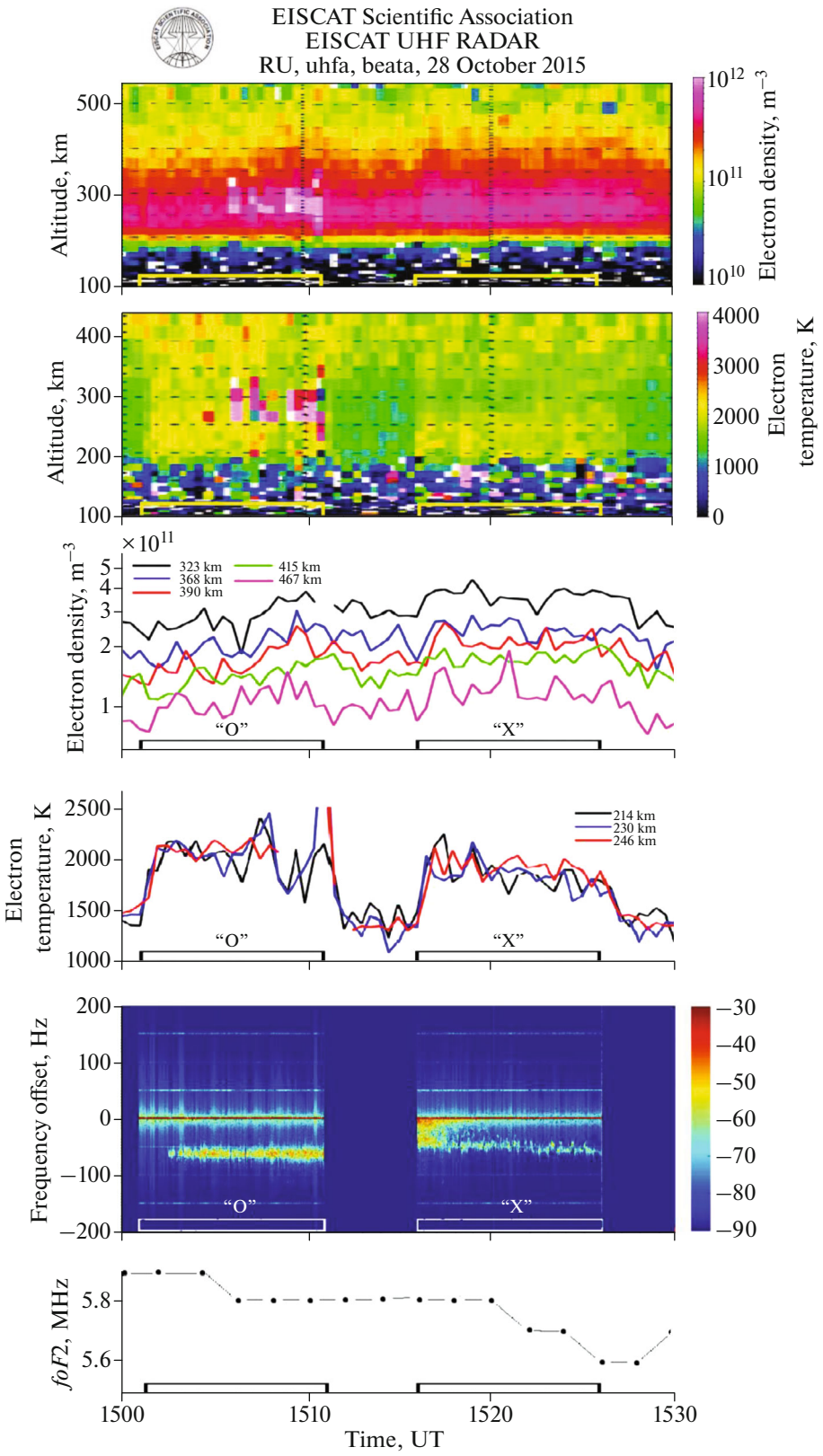

Fig. 2. The altitude-temporal distribution of the electron density *Ne*, m^{-3} and electron temperature *Te*, K, the behavior of *Ne* and *Te* at fixed altitudes, km according to the data measurements of the EISCAT incoherent scatter radar, as well as the NAIRE spectrogram and variations of critical frequencies *foF*2, MHz on October 28, 2015 from 1500 to 1530 UT with alternative O/X heating at f_H = 6.77 MHz. On the NAIRE spectrogram, the frequency offset, Hz is shown on the ordinate axis relative to the heating signal frequency, Hz. The heating cycles and the polarization of the used high-power HF radio wave are marked on the time, UT axis.

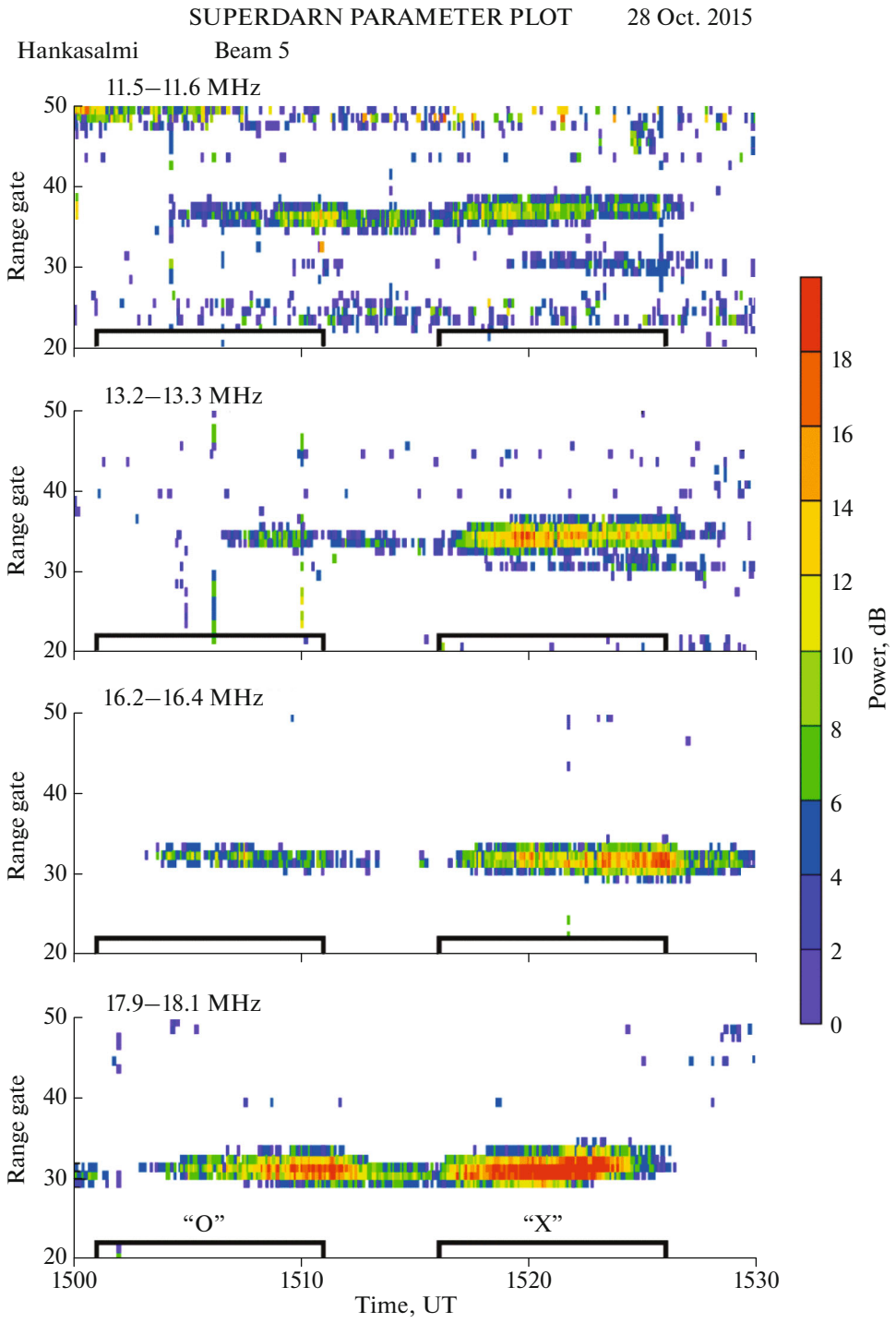

Fig. 3. The powers of signals scattered from SAIIs, dB, at frequencies of $f \sim 11.5$, 13.2, 16.2, and 18 MHz based on data observed by the CUTLASS (SuperDARN) radar at Hankasalmi on beam 5 on October 28, 2015 from 1500 to 1530 UT with alternative O/X, heating at $f_H = 6.77$ MHz. The data are given in the Range gate-time, UT coordinates. The heating cycles and the polarization of the used high-power HF radio wave are marked on the time axis.

was observed due to ohmic heating of electrons, accompanied by a small increase in *Ne*. The behavior of *Ne* at high altitudes (390–467 km) is characterized by two maxima. The first maximum of *Ne* was observed ~2 min after the onset of O heating and was accompanied by the appearance of a discrete component in the NAIRE spectrum that is shifted down in frequency by approximately the gyrofrequency of atomic oxygen ions (O^+ ions). At the same time, SAIIs, which were most intense at 18 MHz ($l_\perp = 8.3$ m), begin

to appear (see Fig. 3). Then, the electron density increased in a wide range of altitudes and reached a maximum at 7–8 min after the onset of the heating cycle. SAIIs with transverse scales to the magnetic field of $l_\perp$ = 8.3–13 m and the discrete component in the NAIRE spectrum after its appearance were recorded during the entire O-heating cycle.

Characteristic features in the behavior of SAIIs in the O-heating cycle from 1501–1511 UT occur the long rise times (2–4 min, depending on the scale of inhomogeneities) and relaxation, which reached the duration of the entire 5-min pause between heating cycles. Such long rise and relaxation times are typical for X-heating when SAIIs in the high-latitude F-region of the ionosphere can be excited upon heating at frequencies both below and above the critical frequency of the *F*2 layer ($f_H \le foF2$ and $f_H > foF2$) (Blagoveshchenskaya et al., 2011, 2015; Blagoveshchenskaya et al., 2019). Thus, the O-wave in the 1501–1511 UT cycle begins to behave as an X-wave. It should be noted that the rise times of SAIIs during X-heating significantly depend on the prehistory of heating ("cold" start in the first X-heating cycle or subsequent X-heating cycles). In X-heating cycles with the prehistory, the influence of after-effects from previous cycles takes over, causing a decrease in the rise time. Precisely this behavior of SAIIs was observed in the next heating cycle (1516–1526 UT) when SAIIs were recorded immediately after turning on the heating stand, but reached their maximum intensity 3–4 min after the start of heating. As can be seen in Fig. 3, the size of the region in which most intense SAIIs were excited was 15 km in both the O- and X-heating cycles. Thus, the behavior and characteristics of SAIIs during O-heating under conditions when the pump wave is not reflected from the ionosphere are typical of inhomogeneities caused by X-heating of the high-latitude *F*-region of the ionosphere.

As follows from Figs. 2 and 3, in the X-heating cycle from 1516 to 1526 UT, an increase in *Ne* was recorded in a wide range of altitudes up to 50% relative to the background values, accompanied by an increase in *Te* up to 30%, generation of the spectral component of NAIRE shifted down in frequency by ~60 Hz, which approximately corresponds to the gyrofrequency of O^+ ions, and intense SAIIs. Such a behavior of *Ne*, *Te*, the spectral structure of NAIRE and SAII is typical for X-heating at frequencies above the critical frequency of the *F*2 layer (Blagoveshchenskaya et al., 2019; Blagoveshchenskaya et al., 2015, 2022; Kalishin et al., 2022).

Thus, as a result of comparing the characteristics of the *Ne* ducts, SAIIs, and the spectral structure of NAIRE during alternative O-/X-heating to the magnetic zenith under conditions when a powerful wave is not reflected from the ionosphere, it was found that, in general, their behavior has the same character while the evolution development of the considered phenomena differs.

3.2. The Experiment at the Heating Frequency f_H = 7.953 MHz

Figure 4 shows the altitude–time distribution of the *Ne* electron density and *Te* temperature, the behavior of *Ne* and *Te* at fixed altitudes according to measurements of the incoherent scatter radar, the NAIRE spectrogram, and variations in the critical frequencies of the *F*2 layer on October 28, 2015 from 1330 to 1400 UT with alternative O/X heating at f_H = 7.953 MHz. As follows from Fig. 4, similarly to the experiment at f_H = 6.77 MHz, a strong increase in the electron density up to 90% (relative to the background values before the onset of heating) in a wide range of altitudes and the generation of a discrete spectral components in the NAIRE spectrum shifted down in frequency by the gyrofrequency of O^+ ions were observed in both O- and X-heating cycles. It should be noted that the growth of *Ne* is smoother in the O-heating cycle compared to that in the X-heating cycle. Thus, upon O-heating, the rise time of *Ne* was ~3.5 min while upon X-heating, it decreased to ~1.5 min.

The emission of a high-power HF radio wave of O-polarization began at 1331 UT when the critical frequency of the *F*2 layer was *foF*2 = 7.4 MHz, which during the first 3 min of heating decreased to *foF*2 = 7.1 MHz and then changed insignificantly within *foF*2 = 7.0– 7.1 MHz until the end of the X-heating cycle at 1356 UT. The fundamental difference between the experiment at the heating frequency of f_H = 7.953 MHz and that considered in Section 3.1 at f_H = 6.77 MHz is that during the first two minutes of the O-heating cycle from 1331 to 1333 UT the reflection of the pump wave from the ionosphere was observed. Figure 5 shows the behavior of the intensities of heat-enhanced plasma lines, as well as ion lines shifted down and up in frequency relative to the HP radar frequency (HF-enhanced plasma lines or HFPL and HF-enhanced downshifted and upshifted ion lines or $HFIL_{DOWN}$ and $HFIL_{UP}$, respectively). As can be seen in Fig. 5, a sharp increase in the altitude of the appearance of HFPL, $HFIL_{DOWN}$, and $HFIL_{UP}$ at 1333 UT indicates the termination of the reflection of a powerful HF radio wave from the ionosphere (the "lights out wave") (see Fig. 5). Under the indicated experimental conditions, the O-wave could not be reflected from the ionosphere and, consequently, cause the excitation of HFPL, $HFIL_{DOWN}$, and $HFIL_{UP}$. However, a wave of extraordinary (X-mode) polarization at f_H = 7.953 MHz can be reflected from the ionosphere above *foF*2 in the frequency range of $foF2 < f_H \le fxF2$, where *fxF*2 is the critical frequency of the extraordinary component of the *F*2 layer. We recall that $fxF2 = foF2 + fce/2$, where *fce* is the electron gyrofrequency. Thus, the X-wave at f_H = 7.953 MHz is reflected from the ionosphere as long as the *foF*2 values remain above 7.25–7.3 MHz. This circumstance is confirmed by the absence of heat-enhanced plasma

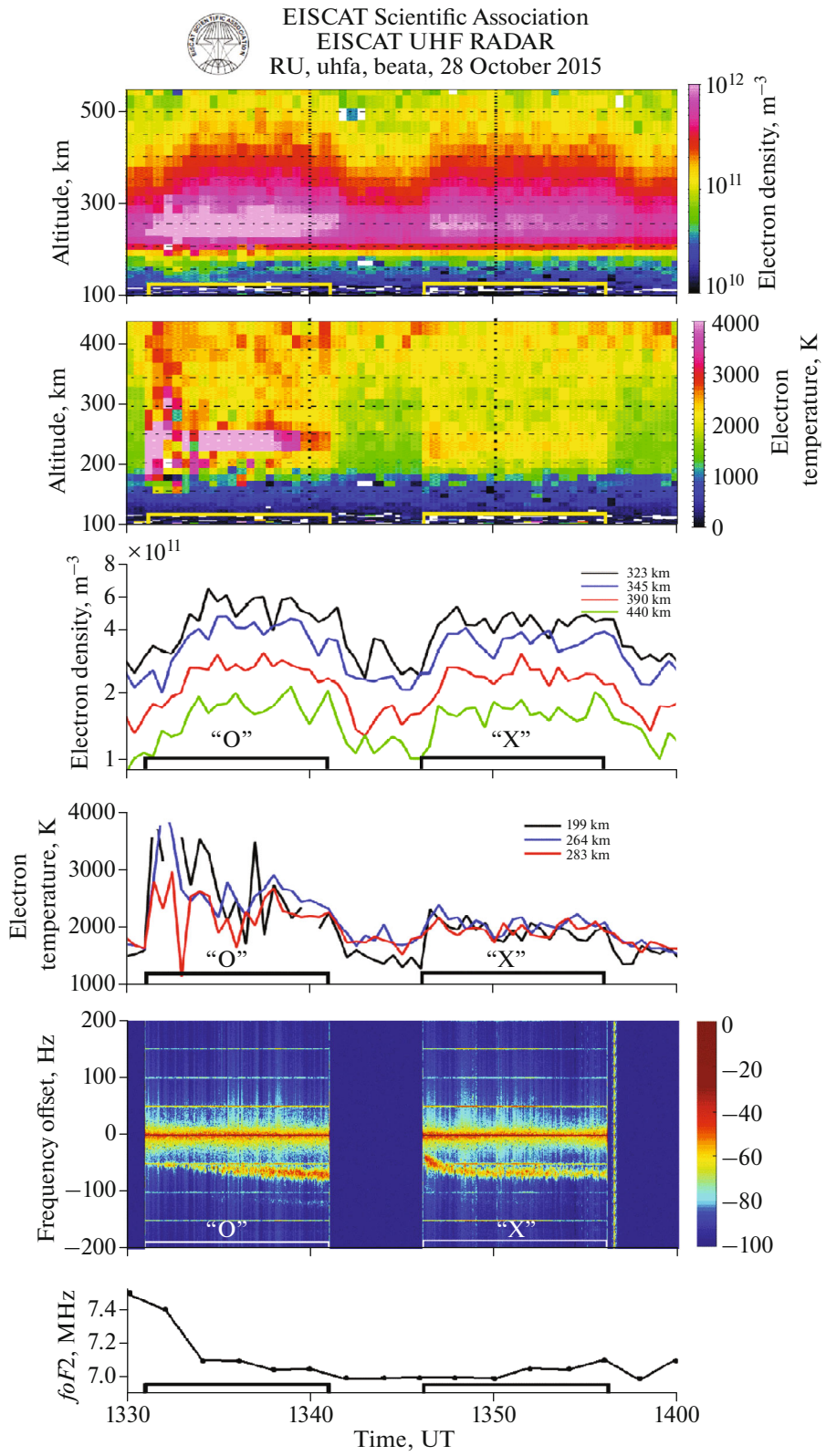

Fig. 4. The altitude-temporal distribution of electron density *Ne*, m^{-3} and electron temperature *Te*, K, the behavior of *Ne* and *Te* at fixed altitudes, km according to the data measurements of the EISCAT incoherent scatter radar, as well as the NAIRE spectrogram and variations of critical frequencies *foF*2, MHz on October 28, 2015 from 1330 to 1400 UT with alternative O/X heating at f_H = 7.953 MHz. On the NAIRE spectrogram, the frequency offset, Hz is shown on the ordinate axis relative to the heating signal frequency, Hz. The heating cycles and the polarization of the used high-power HF radio wave are marked on the time axis (time, UT).

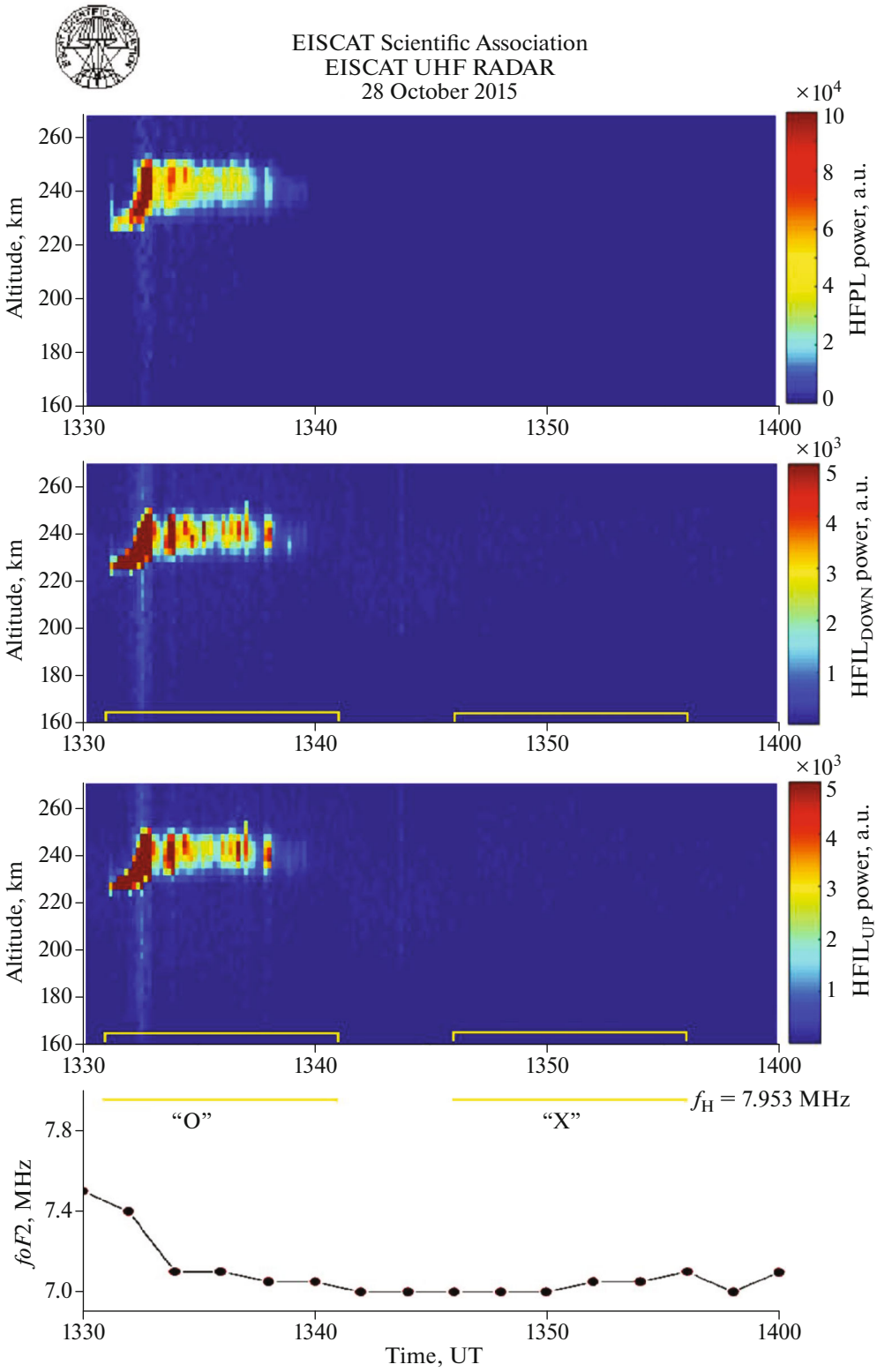

Fig. 5. The behavior of the intensities of heat-enhanced plasma and ion lines (HFPL, $HFIL_{DOWN}$, and $HFIL_{UP}$) in relative units (power, a.u.) in the altitude, km-time, UT coordinates, as well as variations in critical frequencies *foF*2 in MHz October 28, 2015 from 1330 to 1400 UT with alternative O/X heating at $f_H = 7.953$ MHz. The heating cycles and the polarization of the used powerful radio wave are marked on the time axis.

and ion lines, which are direct validation of the excitation of longitudinal plasma waves (Langmuir and ion-acoustic) during X-heating in cycle 1346 to 1356 UT when the values of $foF2$ varied within $foF2$ = 7.0– 7.1 MHz (see Fig. 5).

Comparing the behavior of the electron density *Ne* in a wide range of altitudes and the spectral structure of NAIRE (see Fig. 4), it should be noted that, in general, their behavior during O- and X-heating under conditions when a powerful HF radio wave is not reflected from the ionosphere has the same character.

4. DISCUSSION

According to various means of diagnostics of ionospheric plasma during the period of experiments on the HF heating facility EISCAT/Heating, it was found for the first time that the emission of a high-power HF radio wave of ordinary (O-mode) polarization into the magnetic zenith at frequencies significantly exceeding the critical frequency of the *F*2 layer ($f_H - foF2 = 0.9$–1.1 MHz) leads to the generation of various intense disturbances in the ionospheric plasma. The experiments were performed on October 28, 2015 at heating frequencies of 6.77 and 7.953 MHz at high effective radiation powers (P_{eff} = 350–550 MW). The main observed phenomena under the effect of a high-power HF radio wave of O-polarization under conditions when it is not reflected from the ionosphere include the following: the creation of Ne ducts, the generation of small-scale artificial ionospheric inhomogeneities (SAIIs) and narrow-band artificial ionospheric radio emission (NAIRE). The fact that disturbances are excited in the upper (*F*-region) ionosphere under conditions when a powerful O-wave is not reflected from the ionosphere is unexpected. According to theoretical studies, a powerful HF radio wave of ordinary polarization effectively interacts with ionospheric plasma only when it is reflected from the ionosphere ($f_H \le foF2$) (Gurevich, 1978; Gurevich, 2007; Robinson, 1989; Kuo, 2014). Under these conditions, parametric decay (striction) instability (Perkins et al., 1974; Stubbe et al., 1992; Kuo, 2014) and thermal parametric (resonant) instability (Vaskov and Gurevich, 1975; Grach and Trakhtengerts, 1975) are excited, which lead to the generation of various phenomena in the upper ionosphere.

For comparison, we briefly dwell on the effects of high-power HF radio waves of O- and X-polarization on the high-latitude *F*-region of the ionosphere at heating frequencies below the critical frequency of the *F*2 layer ($f_H \le foF2$). Based on research results (Blagoveshchenskaya et al., 2015, 2020, 2022; Kalishin et al., 2021; Blagoveshchenskaya et al., 2018; Kalishin et al., 2022), it was found that during "classical" O heating at frequencies below the critical frequency of the *F*2 layer ($f_H \le foF2$), *Ne* ducts and NAIRE were not recorded at all while a strong increase in electron temperature *Te* (up to 200–250%) and the generation of intense SAIIs were observed. Typical manifestations of X-heating were an increase in electron density *Ne* (by 50–80% relative to the background) along the magnetic field in a wide range of altitudes up to the upper boundary of the IS radar measurements (600–650 km), the excitation of longitudinal plasma waves (Langmuir and ion-acoustic) during the entire heating cycle, the generation of SAIIs, and narrow-band artificial ionospheric radio emission (NAIRE) that is recorded at a significant (~1200 km) distance from the HF-heating EISCAT/Heating facility. Intense discrete spectral structures and their multiple harmonics shifted down and up in frequency relative to the heating signal frequency that are associated with electrostatic ion-cyclotron waves and their harmonics were found in the NAIRE spectra (Kalishin et al., 2021). The detuning frequencies of these maxima (52–56 Hz) approximately corresponded to the gyrofrequency of O^+ ions and their harmonics (n (52–56) Hz, where n is the harmonic number).

Since, during O-heating SAIIs were excited at frequencies both below and significantly above the critical frequency of the *F*2 layer ($f_H \le foF2$ and $f_H - foF2$ = 0.9–1.1 MHz), it is of interest to consider and compare their characteristics in detail. Figure 6 shows the powers of the signals scattered from SAIIs at frequencies of f ~ 11.5, 13.2, 16.2, 18, and 20 MHz according to observations with the CUTLASS radar during periods of O-heating at f_H = 6.77 MHz. In cycle 1431 to 1441 UT, the pump wave was emitted at $f_H \le foF2$ while at 1501 to 1511 UT, heating was performed under conditions when a powerful O-wave was not reflected from the ionosphere. The data are given in coordinates range(Range gate)-world time, UT. As follows from Fig. 6, at 1431 to 1441 UT, SAIIs excited during O heating at $f_H \le foF2$ appeared/disappeared a few seconds after the heating facility was turned on/off. The size of the region, in which SAIIs were concentrated, was 75 km at radar frequencies of ~18 and 20 MHz ($l_\perp$ = 7.5–8.3 m) and 45 km at frequencies of 11.5, 13.2 and 16.2 MHz ($l_\perp$ = 9.2–13 m). The mechanism of excitation of these inhomogeneities during O-heating is explained by the theory of thermal parametric (resonant) instability (Grach and Trakhtengerts, 1975; Vaskov and Gurevich, 1975; Gurevich, 1978).

The SAII characteristics excited during O-heating at 1501 to 1511 UT under conditions when a powerful HF radio wave was not reflected from the ionosphere fundamentally differ from the case of $f_H \le foF2$, but are in good agreement with the SAII characteristics during X-heating (see Fig. 3). This gives grounds to assume that, at high effective radiation powers at frequencies much higher than $foF2$, the pump O-wave is transformed into an X-wave. Characteristic features in the behavior of SAIIs in the O-heating cycle from 1501 to 1511 UT were the long times of rise (2–4 min, depending on the scale of inhomogeneities) and relax-

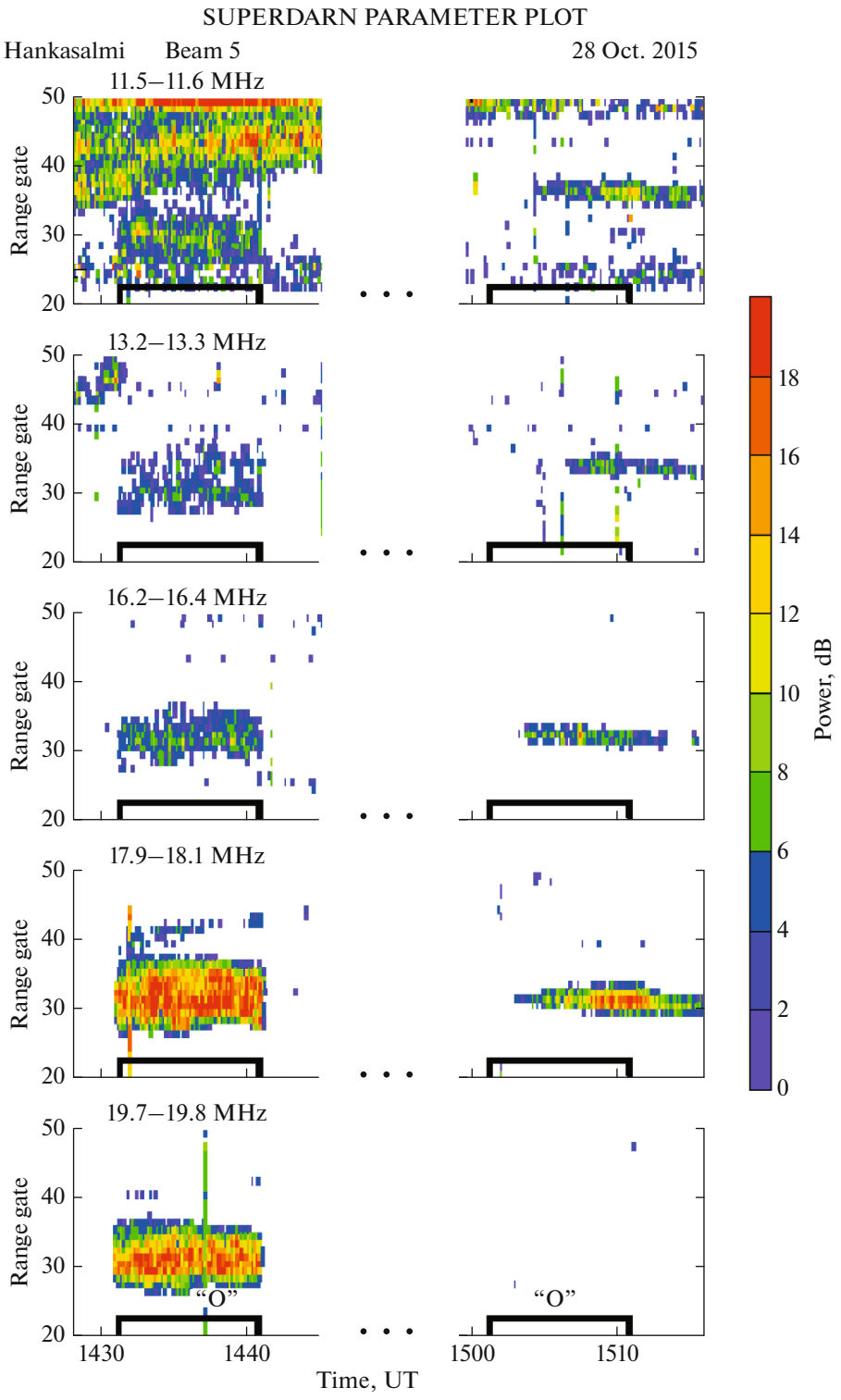

Fig. 6. The powers of signals scattered from SAIIs, dB, at frequencies of $f \sim 11.5$, 13.2, 16.2, 18, and 20 MHz according to observations using the CUTLASS (SuperDARN) radar at Hankasalmi on beam 5 during periods of O-heating at $f_H = 6.77$ MHz. In cycle 1431–1441 UT, the pump wave was emitted at $f_H \le foF2$, and at 1501–1511 UT, heating was performed under conditions when a powerful O-wave was not reflected from the ionosphere. The data are given in Range gate-time, UT coordinates.

ation that reached the duration of the entire 5-min pause, which is typical for X- heating. The rise times of SAIIs significantly depend on the prehistory of heating. In X-heating cycles with a prehistory, the influence of aftereffects from previous cycles is felt, causing a decrease in the rise time of SAIIs, which was observed in the next X-heating cycle from 1516 to 1526 UT (see Fig. 3). The size of the region in which most intense SAIIs were excited under conditions when a powerful wave was not reflected from the ionosphere was 15 km in both the O- and X-heating cycles. The mechanism of excitation of inhomogeneities during O-heating at frequencies significantly exceeding *foF*2, as well as during X-heating at frequencies both above and below *foF*2, can be explained in terms of the Rayleigh–Taylor instability (Kelley, 1989) that develops on horizontal gradients of *Ne* ducts in the presence of an electric field of a powerful HF radio wave orthogonal to the magnetic field. As was shown in (Blagoveshchenskaya et al., 2022), the width of the *Ne* ducts was 3°–4° according to measurements of the incoherent scatter radar in Tromsø that is spatially aligned with the EISCAT/Heating facility. According to the CUTLASS radar, these estimates are in good agreement with the horizontal size of the region occupied by SAIIs, which was ~15 km under conditions when a powerful wave was not reflected from the ionosphere.

We consider in more detail the spectral characteristics of NAIRE during O and X heating at frequencies significantly exceeding the critical frequency of the *F*2 layer ($f_H - foF2 = 0.9–1.1$ MHz). As follows from Figs. 2 and 3, one spectral component was recorded in the NAIRE spectrum for both O and X heating at frequencies of 6.77 and 7.953 MHz in the region of negative detuning from the heating frequency by ~60 Hz, which is close to the gyrofrequency of O^+ ions. A possible mechanism for the generation of this discrete component in the NAIRE spectrum under the effect of a powerful HF radio wave of both ordinary (O-mode) and extraordinary (X-mode) polarization at frequencies significantly exceeding the critical frequency of the *F*2 layer can be stimulated Brillouin scattering (MSBS). Under these conditions, powerful electromagnetic wave EM_0 can directly decay into a scattered electromagnetic wave EM_1 and electrostatic ion cyclotron wave EIC_1: $EM_0 \rightarrow EM_1 + EIC_1$ (Bernhardt et al., 2009, 2010). Then, the conditions for frequency and wave synchronism are represented as follows:

$$\omega_H = \omega_S \pm \omega_{EIC}, \quad k_H = k_S \pm k_{EIC},$$

where ω_H, ω_S, and ω_{EIC} are the frequencies of the pump, scattered, and electrostatic ion-cyclotron waves, respectively; and k_H, k_S, and k_{EIC} are the wave vectors of the pump, scattered, and electrostatic ion-cyclotron waves, respectively.

Based on comparison of the characteristics of the *Ne* ducts, SAIIs, and the spectral structure of NAIRE during alternative O/X heating to the magnetic zenith under conditions when a powerful wave is not reflected from the ionosphere (see Figs. 2, 3, and 4), it was found that, in general, their behavior has the same character and is in good agreement with the results of our other experiments with X heating. This gives grounds to believe that the transformation of an ordinary wave into an extraordinary one occurred under the considered conditions.

5. CONCLUSIONS

It was found for the first time that O-heating of the high-latitude upper ionosphere to the magnetic zenith at high effective radiation powers ($P_{eff} = 350–550$ MW) at frequencies exceeding *foF*2 by 0.9–1.1 MHz leads to the formation of ducts of increased electron density *Ne*, the generation of small-scale artificial ionospheric inhomogeneities (SAIIs), and narrow-band artificial ionospheric radio emission (NAIRE). The behavior and characteristics of SAIIs and the spectral structure of the NAIRE during O-heating under conditions when the pump wave is not reflected from the ionosphere are typical for X-heating of the high-latitude *F*-region of the ionosphere. This indicates that the transformation of an ordinary wave into an extraordinary one occurred under the considered conditions.

The characteristics of *Ne* ducts, SAIIs, and the spectral structure of NAIRE are compared for alternative O-/X-heating to the magnetic zenith at high P_{eff} at frequencies that are significantly higher than the critical frequency of the *F*2 layer. In general, their behavior was established to have the same character, while the evolution of the development and intensity of the considered phenomena is different.

ACKNOWLEDGMENTS

The authors thank the international scientific association EISCAT, which is supported by scientific organizations in China (CRIRP), Finland (SA), Japan (NIPR and STEL), Norway (NFR), Sweden (VR), and the UK (NERC). We are grateful to Prof. T. Yeoman for many years of fruitful cooperation and CUTLASS radar data.

FUNDING

This work was supported by the Russian Science Foundation, project no. 22-17-00020 (https://rscf.ru/project/22-17-00020/).

CONFLICT OF INTEREST

The authors of this work declare that they have no conflicts of interest.

REFERENCES

Ashrafi, M., Kosch, M., Kaila, K., and Isham, B., Spatio-temporal evolution of radio wave pump-induced iono-

spheric phenomena near the fourth electron gyroharmonic, *J. Geophys. Res.*, 2007, vol. 112, p. A05314. https://doi.org/10.1029/2006JA011938

Bernhardt, P.A., Selcher, C.A., Lehmberg, R.H., Rodriguez, S.P., Thomason, J.F., McCarrick, M.J., and Frazer, G.J., Determination of the electron temperature in the modified ionosphere over HAARP using the HF pumped Stimulated Brillouin Scatter (SBS) emission lines, *Ann. Geophys.*, 2009, vol. 27, pp. 4409–4427. https://doi.org/10.5194/angeo-27-4409-2009

Bernhard, P.A., Selcher, C.A., Lehmberg, R.H., Rodriguez, S.P., Thomson, J.F., Groves, K.M., et al., Stimulated Brillouin Scatter in a magnetized ionospheric plasma, *Phys. Rev. Lett.*, 2010, vol. 104, p. 165004. https://doi.org/10.1103/PhysRevLett.104.165004

Blagoveshchenskaya, N.F., Perturbing the high-latitude upper ionosphere (F region) with powerful HF radio waves: A 25-year collaboration with EISCAT, *URSI Radio Sci. Bull.*, 2020, vol. 373, pp. 40–55. https://doi.org/10.23919/URSIRSB.2020.9318436

Blagoveshchenskaya, N.F., Borisova, T.D., Yeoman, T., Rietveld, M.T., Ivanova, I.M., and Baddeley, L.J., Artificial field-aligned irregularities in the high-latitude F region of the ionosphere induced by an X-mode HF heater wave, *Geophys. Res. Lett.*, 2011, vol. 38, p. L08802. https://doi.org/10.1029/2011GL046724

Blagoveshchenskaya, N.F., Borisova, T.D., Kosch, M., Sergienko, T., Brändström, U., Yeoman, T.K., and Häggström, I., Optical and ionospheric phenomena at EISCAT under continuous X-mode HF pumping, *J. Geophys. Res.: Space*, 2014, vol. 119, pp. 10483–10498. https://doi.org/10.1002/2014JA020658

Blagoveshchenskaya, N.F., Borisova, T.D., Yeoman, T.K., Häggström, I., and Kalishin, A.S., Modification of the high latitude ionosphere F region by X-mode powerful HF radio waves: Experimental results from multi-instrument diagnostics, *J. Atmos. Sol.-Terr. Phys.*, 2015, vol. 135, pp. 50–63.

Blagoveshchenskaya, N.F., Borisova, T.D., Kalishin, A.S., Kayatkin, V.N., Yeoman, T.K., and Häggström, I., Comparison of the effects induced by the ordinary (O-mode) and extraordinary (X-mode) polarized powerful HF radio waves in the high-latitude ionospheric *F* region, *Cosmic Res.*, 2018, vol. 56, no. 1, pp. 11–25.

Blagoveshchenskaya, N.F., Borisova, T.D., Kalishin, A.S., Yeoman, T.K., Shmelev, Yu.A., and Leonenko, E.E., Characterization of artificial, small-scale, ionospheric irregularities in the high-latitude *F* region induced by high-power, high-frequency radio waves of extraordinary polarization, *Geomagn. Aeron. (Engl. Transl.)*, 2019, vol. 59, no. 6, pp. 713–725.

Blagoveshchenskaya, N.F., Borisova, T.D., Kalishin, A.S., Yeoman, T.K., and Häggström, I., Distinctive features of Langmuir and ion-acoustic turbulences induced by O- and X-mode HF pumping at EISCAT, *J. Geophys. Res.: Space*, 2020, vol. 125. https://doi.org/10.1029/2020JA028203

Blagoveshchenskaya, N.F., Borisova, T.D., Kalishin, A.S., Egorov, I.M., and Zagorskiy, G.A., Disturbances of electron density in the high latitude upper (F-region) ionosphere induced by X-mode HF pump waves from EISCAT UHF radar observations, *Probl. Arkt. Antarkt.*, 2022, vol. 68, no. 3, pp. 248–257. https://doi.org/10.30758/0555-2648-2022-68-3-248-257

Dhillon, R.S. and Robinson, T.R., Observations of time dependence and aspect sensitivity of regions of enhanced UHF backscatter associated with RF heating, *Ann. Geophys.*, 2005, vol. 23, pp. 75–85.

Frolov, V.L., *Iskusstvennaya turbulentnost' sredneshirotnoi ionosfery* (Artificial Turbulence of the Midlatitude Ionosphere), Nizhny Novgorod: Nizhegorod. univ., 2017.

Grach, S.M. and Trakhtengerts, V.Yu., Parametric excitation of ionospheric irregularities extended along the magnetic field, *Radiophys. Quantum Electron.*, 1975, vol. 18, pp. 951–957.

Gurevich, A.V., *Nonlinear Phenomena in the Ionosphere*, New York: Springer, 1978.

Gurevich, A.V., Nonlinear effects in the ionosphere, *Phys.-Usp.*, 2007, vol. 50, no. 11, pp. 1091–1122. https://doi.org/10.1070/PU2007v050n11ABEH006212

Hagfors, T., Kofman, W., Kopka, H., Stubbe, P., and Ijnen, T., Observations of enhanced plasma lines by EISCAT during heating experiments, *Radio Sci.*, 1983, vol. 18, pp. 861–866.

Kalishin, A.S., Blagoveshchenskaya, N.F., Borisova, T.D., and Rogov, D.D., Remote diagnostics of effects induced by high-latitude heating facilities, *Russ. Meteorol. Hydrol.*, 2021a, vol. 46, no. 4, pp. 231–240. https://doi.org/10.3103/S1068373921040038

Kalishin, A.S., Blagoveshchenskaya, N.F., Borisova, T.D., and Yeoman, T.K., Ion gyro-harmonic structures in stimulated emission excited by X-mode high power HF radio waves at EISCAT, *J. Geophys Res.: Space*, 2021b, vol. 126, p. e2020JA028989. https://doi.org/10.1029/2020JA028989

Kalishin, A.S., Blagoveshchenskaya, N.F., Borisova, T.D., and Egorov, I.M., Comparison of spectral features of narrowband stimulated electromagnetic emission excited by an extraordinary pump wave in the high-latitude ionospheric F region at frequencies below and above the F2 layer X-component critical frequency, *Russ. Meteorol. Hydrol.*, 2022, vol. 47, no. 4, pp. 921–930.

Kelley, M.C., *The Earth's Ionosphere: Plasma Physics and Electrodynamics*, San Diego, Calif.: Academic Press, 1989.

Kuo, S.P., Overview of ionospheric modification by High Frequency (HF) heaters: Theory, *Progr. Electromagn. Res. B*, 2014, vol. 60, pp. 141–155.

Lehtinen, M.S. and Huuskonen, A., General incoherent scatter analysis and GUISDAP, *J. Atmos. Sol.-Terr. Phys.*, 1996, vol. 58, pp. 435–452.

Lester, M., Chapman, P.J., Cowley, S.W.H., et al., Stereo CUTLASS: A new capability for the SuperDARN radars, *Ann. Geophys.*, 2004, vol. 22, no. 2, pp. 459–473.

Mishin, E., Watkins, B., Lehtinen, N., Eliasson, B., Pedersen, T., and Grach, S., Artificial ionospheric layers driven by high-frequency radiowaves: An assessment, *j. Geophys. Res., Space*, 2016, vol. 121. https://doi.org/10.1002/2015JA021823

Pedersen, T., Gustavsson, B., Mishin, E., Kendall, E., Mills, T., Carlson, H.C., and Snyder, A.L., Creation of

artificial ionospheric layers using high-power HF waves, *Geophys. Res. Lett.*, 2010, vol. 37, p. L02106. https://doi.org/10.1029/2009GL041895

Pedersen, T., McCarrick, M., Reinisch, B., Watkins, B., Hamel, R., and Paznukhov, V., Production of artificial ionospheric layers by frequency sweeping near the 2nd gyroharmonic, *Ann. Geophys.*, 2011, vol. 29, pp. 29–47. https://doi.org/10.5194/angeo-29-47-2011

Perkins, F.W., Oberman, C., and Valco, E.J., Parametric instabilities and ionospheric modification, *J. Geophys. Res.*, 1974, vol. 79, pp. 1478–1496.

Rietveld, M.T., Senior, A., Markkanen, J., and Westman, A., New capabilities of the upgraded EISCAT high-power HF facility, *Radio Sci.*, 2016, vol. 51, no. 9, pp. 1533–1546. https://doi.org/10.1002/2016RS006093

Rishbeth, H. and van Eyken, T., EISCAT: Early history and the first ten years of operation, *J. Atmos. Sol.-Terr. Phys.*, 1993, vol. 55, pp. 525–542.

Robinson, T.R., The heating of the high latitude ionosphere by high power radio waves, *Phys. Rep.*, 1989, vol. 179, pp. 79–209.

Stubbe, P., Review of ionospheric modification experiments at Tromsø, *J. Atmos. Sol.-Terr. Phys.*, 1996, vol. 58, pp. 349–368.

Stubbe, P., Kohl, H., and Rietveld, M.T., Langmuir turbulence and ionospheric modification, *J. Geophys. Res.*, 1992, vol. 97, pp. 6285–6297.

Vas'kov, V.V. and Gurevich, A.V., Nonlinear resonant instability of a plasma in the field of an ordinary electromagnetic wave, *J. Exp. Theor. Phys.*, 1975, vol. 42, no. 1, pp. 91–97.

Yeoman, T.K., Blagoveshchenskaya, N.F., Kornienko, V.A., Robinson, T.R., Dhillon, R.S., Wright, D.M., and Baddeley, L.J., SPEAR: Early results from a very high latitude ionospheric heating facility, *Adv. Space Res.*, 2007, vol. 40, pp. 384–389.

Translated by A. Ivanov